P1.15

Examining the aerosol indirect effect in the second aerosol characterization experiment (ACE-2) with a cloud resolving model

Huan Guo*, Joyce E. Penner and Michael Herzog

University of Michigan, Ann Arbor, MI, 48109, USA

1. Introduction

Many anthropogenic aerosols are effective cloud condensation nuclei (CCN), and can influence the cloud droplet number concentration (CDNC). For a given cloud water content, a larger CDNC means a smaller droplet size, i.e., the so-called first Aerosol Indirect Effect (AIE)[*Twomey*, 1977]. Moreover, it is more difficult for the smaller cloud droplets to grow large enough and fall down as precipitation, which can lead to larger liquid water path, i.e., the so-called second AIE [*Albrecht*, 1989]. Based on the current model estimates, the indirect aerosol forcing ranges from 0.0 to -4.8 W/m^2 [*Penner et al.*, 2001], which can potentially counteract the warming caused by greenhouse gases. Therefore, it is important to study the aerosol-cloud interactions further.

The second Aerosol Characterization Experiment (ACE-2) offers a good opportunity to study the impact of aerosols on marine stratocumulus clouds [*Raes et al.*, 2000]. ACE-2 took place from 16 June to 24 July, 1997, over the subtropical northeast Atlantic. Previous observations showed that the clean marine air alternates with the anthropogenic pollution over this area. The CLOUDY-COLUMN (CC) experiment, one of 6 field projects during ACE-2, was set up to study the effects of aerosol on the microphysical and radiative properties of marine boundary layer clouds [*Raes et al.*, 2000; *Brenguier et al.*, 2000]. However, the individual contribution from the aerosols or from the meteorological conditions can not be distinguished from the field experiment. To date, no study has used a cloud resolving model (CRM) to examine the possible aerosol indirect effects on marine stratocumulus clouds in the contrasting aerosol conditions that occurred during the ACE-2 experiment.

In this study, a cloud resolving model, ATHAM (Active Tracer High Resolution Atmospheric Model), is used to study the aerosol indirect effect in contrasting clean (26 June) and polluted environments (9, July). These two days provide conditions with significant differences in the cloud droplet effective radius (r_v), the cloud droplet number concentration (CDNC), and the averaged precipitation rate within the cloud layers (PR) [*Pawlowska and Brenguier*, 2003].

2. Model description and simulation setup

ATHAM is a non-hydrostatic, fully compressible atmospheric circulation model, formulated with an implicit-time step and finite-difference scheme [*Oberhuber et al.*, 1998; *Herzog et al.*, 2003]. Periodic lateral boundary conditions are adopted [*Tao et al.*, 1987]. For the lower boundary, a material surface is assumed, across which surface heat and moisture fluxes can pass. At the model top, a rigid lid is assumed. To minimize the spurious reflection of the upward propagating gravity waves, a sponge layer is applied at the upper part of the numerical domain (upper 8% of the vertical levels).

The simulations used 121×150 grids covering a numerical domain of 242km×20km. The horizontal resolution is uniformly set to be 2km, and the vertical resolution is 40m for the first 3.2km, above which the resolution is stretched to about 300m at the top of the domain. The center of the domain is taken as equal to the location of the observations during the ACE-2 experiment (29.4N, 16.7W). For the imposition of the large-scale forcing, *Grabowski*'s strategy [1996] is followed except that, only the horizontal large-scale advection, instead of the sum of the horizontal and vertical advections, are applied for the potential temperature and specific humidity. According to *Grabowski*'s strategy [1996], the domain averaged horizontal momentum fields are nudged toward the large-scale background horizontal momentum fields with a relaxation timescale of 1 hour. The European Center for Medium-Range Weather Forecasts (ECMWF) reanalysis data has been interpolated to the model height levels and time intervals, which provides the time-dependent background horizontal momentum fields, pressure, large-scale horizontal temperature and moisture advections, and surface temperature.

The effect of aerosols on clouds is initiated through the nucleation of cloud droplets by aerosols. Cloud Condensation Nuclei (CCN) are activated in response to the supersaturation produced in an updraft, mainly at the cloud base. This activation process relates the initial cloud droplet number concentration (CDNC) with the aerosol composition, size distribution and number concentration. In this study, the Chuang and Penner nucleation scheme [1995] is adopted.

$$Q_{act} = max(\frac{wN_a}{w + \alpha N_a} - N_{old}, 0). \quad (1)$$

In the *Chuang and Penner* scheme, the activation of aerosol (Q_{act}) depends on the total number of hygroscopic aerosols (N_a), the updraft velocity (w) and a factor of α, which takes the aerosol composition and size spectrum into account [*Chuang and Penner*, 1995]. N_{old} in Eq.(1) is the number of cloud droplets present before the current time step.

In ATHAM, cloud microphysical parameterization follows Kessler-type bulk scheme except for the auto-conversion and accretion processes, for which, Beheng's scheme is adopted [*Herzog*, 1998; *Kessler*, 1969; *Beheng*, 1994].

* *Corresponding author address:* Huan Guo, 1546 SRB, 2455 Hayward St., Ann Arbor, MI, 48109-2143.
E-mail: hguo@umich.edu

The shortwave radiation parameterization uses a delta-Eddington approximation. It has 9 bands covering the Ultra-Visible (UV) and visible region from 0.175 μm to 0.700 mum and 3 bands resolving H_2O absorption in the near Infra-Red (IR) between 0.7 and 4.0 μm [*Grant et al.*, 1998]. 13 aerosol species (mainly fossil fuel, biomass burning, sea salt and dust) and the dependence of their optical properties on relative humidity are taken into account [*Grant et al.*, 1999]. The longwave radiation code includes parameterizations for the absorption of H_2O, O_3, CO_2 and for most of the minor trace gases (N_2O, CH_4, CFC′s), as well as the radiative effects of warm clouds [*Chou et al.*, 2001].

3. Numerical results

The second Aerosol Characterization Experiment (ACE-2) took place over the sub-tropical northeast Atlantic (29.4N, 16.7W). This region was characterized by a strong temperature inversion, which separates the marine boundary layer (MBL) from the upper free troposphere (FT). Observations indicate that in the MBL, clean air alternates with anthropogenic pollution from Europe and North America, while in the free troposphere, clean air masses alternate with mineral dust from North Africa [*Verver et al.*, 2000]. Therefore, this region provides a good opportunity to investigate the interaction between anthropogenic aerosols and stratiform clouds forming at the top of the MBL.

The CLOUDY COLUMN (CC) project of the ACE-2 experiment consists of 8 cases; 2 clean, 3 polluted and 3 intermediate cases. Two cases on June 26 and July 9 are studied here. On June 26, the air was originally from the ocean (relatively clean). We denote this as the 'clean' case. On July 9, there was a large amount of aerosol from continental Europe. We denote this as the 'polluted' case. Measurements are available around local noon. Table 1 presents the observed cloud microphysical and radiative properties of these two cases [*Menon et al.*, 2003; *Pawlowska and Brenguier*, 2003]. From the observation data, we can see that the Cloud Droplet Number Concentration (CDNC), the volume mean cloud droplet radius (r_v) and the averaged precipitation rate within the cloud layers (PR) exhibit significant differences between the clean and polluted cases.

3.1. Base Case

Initial conditions were obtained from the ECMWF reanalysis data. The model was run for a 30-hour period. For example, the simulation began at 18Z, June 25 (local time), and ended at 00Z, June 27 in the clean case. The first 6 hours of the simulation was used to spinup the model and let clouds form. After the 6-hour spinup, the simulated vertical profiles of the temperature and specific humidity are consistant with the aircraft measurements. In the following we mainly discuss the last 24 hours of the simulations.

Table 1. Cloud microphysical and radiative properties of the clean (26 June) and polluted (9, July) cases[a]

	clean (26 June)	polluted (9, July)
CDNC (cm^{-3})	52±16	256±38
r_v (μm)	7.77±3.64	4.73±1.67
LWP (g/m^2)	18.5±17.8	11.0±10.8
COD	3.99±2.29	4.23±2.54
CF	87%	50%
PR ($\mu g/m^2/s$)	25.5	2.22

[a] Parameters as defined in Section 3.

Our first concern is whether ATHAM can reproduce the observed cloud microphysical and radiative properties. Figures 1 and 2 show the simulated mean LWP, CDNC, r_v and Cloud Optical Depth (COD, τ) within the cloud layers, and their associated standard deviations (shaded area) [1]. The mean values and their standard deviations from observations around local noon are denoted as '*' and vertical lines, respectively.

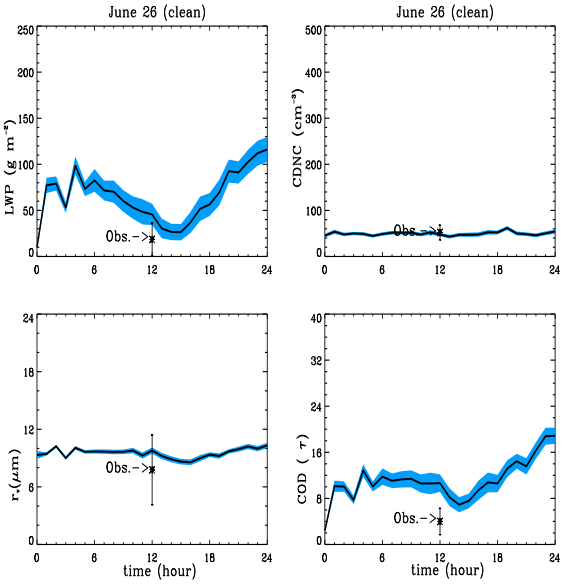

Figure 1. The time-evolution of the cloud mean LWP, CDNC, r_v, COD (τ) from ATHAM (solid line) and their standard deviations (shaded area), as well as from the observations (mean and standard deviation) around local noon in the clean case (26, June).

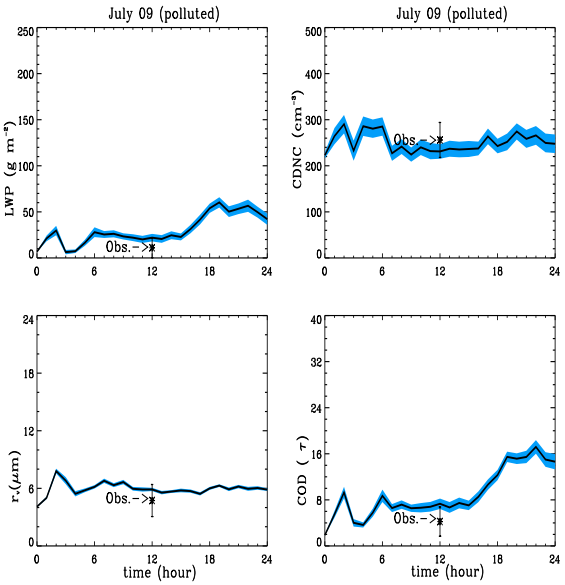

Figure 2. The same as Figure 1, but for the polluted case (9, July).

The predicted mean CDNC and r_v in both cases are well within the observational uncertainties. The LWPs and

CODs are within the range of the standard deviations in the polluted case, but close to the upper end of the standard deviation in the clean case. This moist bias may be caused by the lack of large-scale advection for the liquid water to remove excess liquid water out of the cyclic domain [*Grabowski et al.*, 1996]. Though other causes are also being investigated.

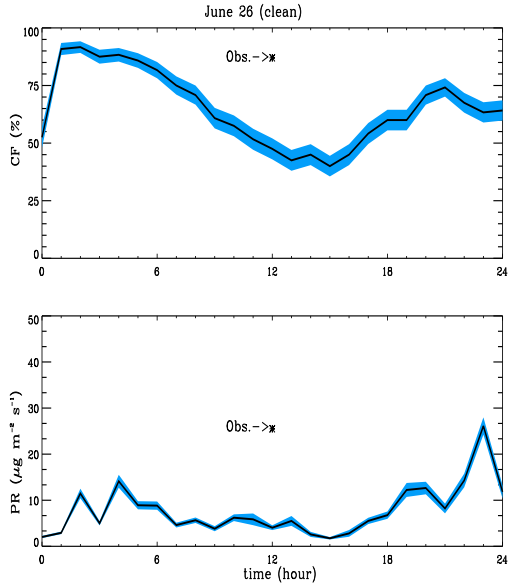

Figure 3. The time-evolution of the mean CF and PR from ATHAM (solid line) and their standard deviation (shaded area), as well as from the observations (mean) around local noon in the clean case (26, June).

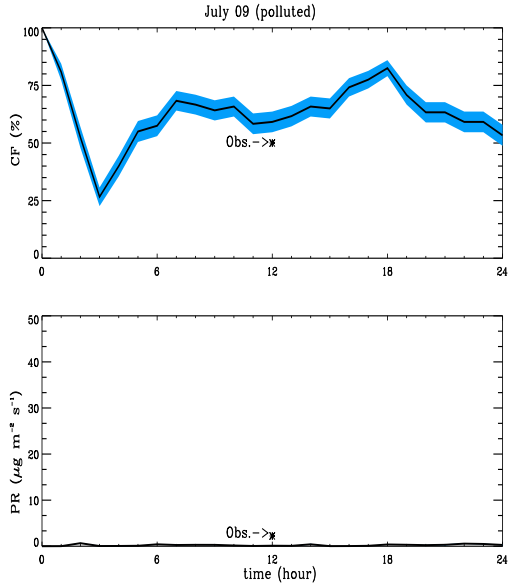

Figure 4. The same as Figure 3, but for the polluted case(9, July).

For the CF and PR, only observed mean values are available in both the clean and polluted cases, denoted as '*' in Figures 3 and 4. The shaded area in Figures 3 and 4 presents the standard deviation of the simulation results. The observed PRs are larger than those simulated in both the clean and the polluted cases by a factor of about 5. This discrepancy might be explained as follows. The observational data for the mean precipitation rate was retrieved from measurements of the drop size distribution and number concentration. Since drizzle particles are sparse, the statistical significance for the observation is low and the estimated precipitation rate has a large uncertainty [*Pawlowska and Brenguier*, 2003]. *Menon et al* [2003] noted that the observed flux could be overestimated by a factor of 5 to 10. On the other hand, the rain drops in ATHAM are assumed to follow the Marshall-Palmer distribution. For the drizzle particles, it might not be a good approximation [*Zawadzki et al.*, 1994; *Rogers and Yau*, 1989], which might result in a biased prediction of the PR in the simulations.

In the clean case (26, June), the simulated cloud LWP, COD, CF, and PR exhibit significant diurnal changes. At night, the LWP and COD are larger than during the daytime when the short-wave radiation heating evaporates the droplets and dissipates the clouds. However this is not true for the polluted case (9, July), where the diurnal variation is not as significant as in the clean case. During the CC experiment, a mid-latitude cyclone and a high pressure system alternated to influence the ACE-2 area. On June 26, the ACE-2 area was under the influence of a cyclone, which brought marine clean air to the experimental site. But on July 9, a high pressure system was responsible for transporting anthropogenic pollution from Europe to the ACE-2 area. Hence, clouds show a significant diurnal variation in the clean case (26, June), but in the polluted case (9, July), the diurnal variation is masked by the influence of the high pressure system [*Verver et al.*, 2000; *Menon et al.*, 2003].

Comparing Figure 1 and Figure 2, we can see that the CDNC and r_v differ significantly between the clean and polluted cases although the LWPs are similar around local noon. In the clean case, the aerosol number concentration is 210 cm^{-3}; while it is 580 cm^{-3} in the polluted case. This difference leads to different CDNCs, which are about 50 cm^{-3} and 250 cm^{-3} in the clean and polluted cases, respectively. The PR is larger in the clean case (see Figures 3 and 4). As discussed above, r_v in the polluted case (about $5\mu m$) is only about half of that in the clean case (about $10\mu m$). Therefore, only a very few droplets can be larger than the critical threshold r_0(10 μm here) to allow autoconversion to occur. As a result, the PR is low in the polluted case.

4. Sensitivity test

4.1. Swapping aerosol data between the clean and polluted cases

The aerosol loading is exchanged between the clean and polluted cases. In the test CL_Met/PO_Ars (the Clean Meteorological condition with Polluted Aerosol loading), the initial condition and large-scale forcing are the same as in the clean case (26, June), but the polluted aerosol information is used (9, July). In the test PO_Met/CL_Ars (the Polluted Meteorological condition with Clean Aerosol loading), the initial condition and large-scale forcing are the same as in the polluted case (9, July), but the clean aerosol information is used (26, June).

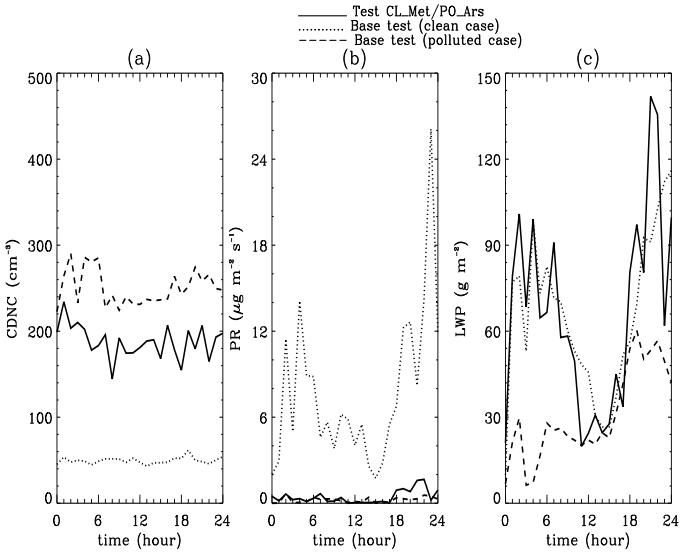

Figure 5. The time-evolution of LWP, CDNC and PR in the Test CL_Met/PO_Ars (solid line), which combines the initial conditions and large-scale forcing of the clean case with the aerosol loading of the polluted case, and in base cases for the clean case (26, June) (dotted) and the polluted case (9, July) (dash line).

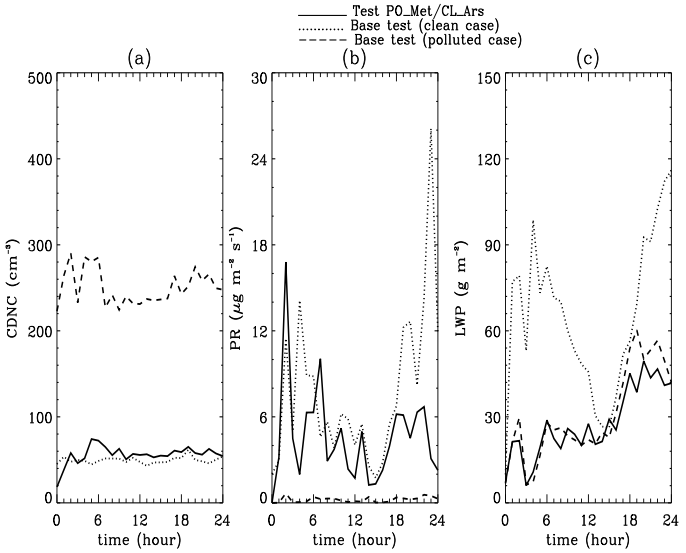

Figure 6. The same as Figure 5, but for the Test PO_Met/CL_Ars (solid line), which combines the initial conditions and large-scale forcing of the polluted case with the aerosol loading of the clean case.

The results of test CL_Met/PO_Ars and test PO_Met/CL_Ars are shown in Figures 5 and 6. It is interesting to note two points here. First is that the time evolution of CDNC and PR in the test CL_Met/PO_Ars generally follow those of the polluted case, but in the test PO_Met/CL_Ars they follow the clean case. The CDNC and PR are closely related with the environmental aerosol loading. Second is that the LWP in test CL_Met/PO_Ars compares favorably with that of the clean case, but in the test PO_Met/CL_Ars it agrees well with the polluted case. The LWP is not sensitive to the aerosol amount, but instead is related to the meteorological conditions, more specifically, the surface vapor flux.

5. Conclusions

A cloud resolving model, ATHAM, has been adopted to test against the clean and polluted cases in the CLOUDY COLUMN project of the ACE-2 experiment. To evaluate the performance of ATHAM, the model outputs are compared with the field measurements. The general cloud features from ATHAM are well within the observational uncertainties. The LWP and COD are close to or within the upper bound of the standard deviation of the observations. This moist bias might be interpreted by the combination of the cyclic boundary condition and lack of the large-scale forcing term for liquid water [*Grabowski et al.*, 1996].

In the clean case, the cloud properties exhibit a significant diurnal variation. But in the polluted case, they do not. In addition, the CDNC, droplet size and precipitation efficiency differ a lot. The test CL_Met/PO_Ars and test PO_Met/CL_Ars imply that the difference is caused by the different aerosol loadings. The cloud CDNC, droplet size and precipitation efficiency are sensitive to the different aerosol amounts, but insensitive to the different meteorological backgrounds. The LWP is sensitive to the meteorological background, but insensitive to the aerosol amount.

Acknowledgments. This work was supported by the DOE ARM program and the Ford University Research Fund (URP).

Notes

1. Here the mean ($\overline{X}$) and its standard deviation ($\overline{\sigma}$) are $\overline{X} = \frac{1}{N}\sum_{i=1}^{N} X_i$, $\overline{\sigma} = \sqrt{\sum_{i=1}^{N} \frac{(X_i - \overline{X})^2}{N(N-1)}}$, where N is the number of the column where the cloud exists

References

Albrecht, B. (1989), Aerosols, cloud microphysics, and fractional cloudiness, *Science,*, *243*, 1227–1230.

Beheng, K. (1994), A parameterization of warm cloud microphysical conversion processes, *Atmos. Res.,*, *33*, 207–233.

Brenguier, J.-L., P. Chuang, Y. Fouquart, D. Johnson, and et al. (2000), An overview of the ace-2 cloudycolumn closure experiment, *Tellus,*, *52B*, 815–827.

Chou, M., M. Suarez, X. Liang, and M.-H. Yan (2001), A thermal infrared radiation parameterization for atmospheric studies, *Tech. Rep. on global modeling and data assimilation, NASA/TM-2001-104606, Vol.19*, Goddard Space Flight Center.

Chuang, C., and J. Penner (1995), Effect of anthropogenic sulfate on cloud drop nucleation and optical properties, *Tellus,*, *47B*, 566–577.

Grabowski, W., X. Wu, and M. Moncrieff (1996), Cloud resolving modeling of tropical systems during phase iii of gate. part i two-dimensional experiments, *J. Atmos. Sci.,*, *53*, 3684–3709.

Grant, K., A. Grossman, C. Chuang, and J. Penner (1998), *Description of a solar radiative transfer model for use in LLNL climate and atmospheric chemistry studies*, lawrance Livermore National Laboratory (LLNL) Report UCID-ID-129949. (Available online as an Adobe Acrobatz PDF file under http//www.llnl.gov/llnl_only/tid/lof/documents/pdf/233048.pdf).

Grant, K., C. Chuang, A. Grossman, and J. Penner (1999), Modeling the spectral optical properties of ammonium sulfate and biomass burning aerosols; parameterization of relative humidity effects and model results, *Atmospheric Environment,*, *33*, 2603–2620.

Herzog, M. (1998), Simulation der Dynamik eines Multikomponentensystems am Beispiel vulkanischer Eruptionswolken, Ph.D. thesis, Max - Planck - Institute for Meteorology, Hamburg, Germany.

Herzog, M., J. M. Oberhuber, and H. Graf (2003), A prognostic turbulence scheme for the non-hydrostatic plume model, *J. Atmos. Sci.,*, *60*, 2783–2796.

Kessler, E. (1969), On the distribution and continuity of water substance in atmospheric circulation, *Met. Monographs,*, *10*, 84.

Menon, S., J.-L. Brenguier, O. Boucher, P. Davison, and et al. (2003), Evaluating aerosol/cloud/radiation process parameterizations with single-column models and second aerosol characterization experiment (ace-2) cloudy column observations, *J. Geophys. Res.,*, *108*(D24), 4762, doi:10.1029/2003JD003,902.

Oberhuber, J. M., M. Herzog, H.-F. Graf, and K. Schwanke (1998), Volcanic plume simulation on large scales, *J. Volcanol. Geotherm. Res.,*, *87*, 29–53.

Pawlowska, H., and J.-L. Brenguier (2003), An observational study of drizzle formation in stratocumulus clouds for general circulation model (gcm) parameterizations, *J. Geophys. Res.,*, *108*(D15), 8630, doi10.1029/2002JD002,679.

Penner, J. E., et al. (2001), *Climatic Change 2001 The Scientific Basis*, chap. 5 Aerosols, their direct and indirect effects, pp. 289–348, Cambridge University Press, ed. by J. T. Houghton and Y. Ding and D. J. Griggs and M. Noguer and P.J. van der Linden and X. Dai and K. Maskell and C. A. Johnson, Report to Intergovernmental Panel on Climate Change from the Scientific Assessment Working Group (WGI).

Raes, F., T. Bates, F. Mcgovern, and M. Van-Liedekerke (2000), The 2nd aerosol characterization experiments (ace-2) general overview and main results, *Tellus,*, *52B*, 111–125.

Rogers, R., and M. Yau (1989), *A short course in cloud physics*, Butterworth-Heinemann Publication, Woburn, MA.

Tao, W.-K., J. Simpson, and S.-T. Soong (1987), Statistical properties of a cloud ensemble a numerical study, *J. Atmos. Sci.,*, *44*, 3175–3187.

Twomey, S. (1977), The influence of pollution on the shortwave albedo of clouds, *J. Atmos. Sci.,*, *34*, 1149–1152.

Verver, G., F. Raes, D. Vogelezang, and D. Johnson (2000), The 2nd aerosol characterization experiment (ace-2) meteorological and chemical context, *Tellus,*, *52B*, 126–140.

Zawadzki, I., D. Monteiro, and F. Fabry (1994), The developement of drop size distributions in light rain, *J. Atmos. Sci.,*, *51*, 1100–1113.